
THE MINIMUM OF THE TIME-DELAY WAVEFRONT ERROR IN ADAPTIVE OPTICS

A PREPRINT

Niek Doelman*

Department of Opto-Mechatronics
TNO Industry
Delft, The Netherlands
niek.doelman@tno.nl

February 28, 2022

ABSTRACT

An analytical expression is given for the minimum of the time-delay induced wavefront error (also known as the servo-lag error) in Adaptive Optics systems under temporal prediction filtering. The analysis is based on the von Kármán model for the spectral density of refractive index fluctuations and the hypothesis of frozen flow. An optimal, temporal predictor can achieve up to a factor 1.77 more reduction of the wavefront phase variance compared to the zero-order prediction strategy, which is commonly used in Adaptive Optics systems. Alternatively, an optimal predictor can allow for a 1.41 times longer time-delay to arrive at the same residual phase variance. Generally, the performance of the optimal, temporal predictor depends on the very product of time-delay, wind speed and the reciprocal of turbulence outer scale.

Keywords Atmospheric Turbulence · Adaptive Optics

1 Introduction

- The residual wavefront error of an astronomical imaging instrument equipped with an Adaptive Optics (AO) system, is determined by several error sources. The instrumental-type errors represent the limitations of the AO system components to cancel the turbulence-induced wavefront distortion. One of the most prominent instrumental AO error sources is the time-delay error, which is due to the overall latency between the sensing and the actual correction of the wavefront. This error is also known as the AO servo-lag error.

In [1] the impact of the time-delay on the residual AO wavefront error has been described. A specific analytical expression is given for the wavefront error variance, for Kolmogorov turbulence and at a single point. The time-delay analysis is based on a control approach, of which the essence is to feed the latest (measured) wavefront phase value, with opposite sign, back to the optical wavefield. In continuous-time notation, this control action leads to the residual phase:

$$\epsilon_{ref}(t) = \phi(t + \Delta t) - \phi(t) \quad (1)$$

in which $\phi(t)$ represents the wavefront phase fluctuations as a function of time t , Δt the time-delay and $\epsilon_{ref}(t)$ the residual phase. This control strategy is very common in AO systems and is denoted as *zero-order prediction* in [2]. For the remainder of the paper it will be denoted as the reference approach.

In practice, many closed-loop AO systems utilise the zero-order prediction strategy, in the form of a discrete-time integrator. It needs to be noted that the integrator, as a result of the closed-loop stability constraint, may not obtain the same performance as the zero-order prediction strategy.

*2nd affiliation: Leiden Observatory, Leiden University, The Netherlands.

The variance of the residual wavefront error for the reference prediction approach ([1]) is evaluated as

$$\sigma_{ref}^2 = 28.4(f_G \Delta t)^{5/3} \quad (2)$$

with f_G the Greenwood frequency.

This analytical expression is often used in AO performance analysis, design and error budgeting. The underlying reference controller has the advantage of having the lowest possible order and being straightforward to implement. Yet, it does not achieve the minimum possible value of the mean square time-delay error.

1.1 Optimal prediction

More advanced prediction methods to reduce the effect of the AO time-delay have been proposed by various researchers. In particular, optimal prediction has gained a lot of attention since it aims at achieving the minimum of the mean square phase error. In ([3]) this principle is proposed in the context of AO within a closed-loop Linear Quadratic Gaussian control approach. Since then, optimal prediction for AO has been discussed by many authors; see for instance ([4]) for a recent overview and references therein. The large majority of the work on AO predictive control has been focused on numerical simulations, laboratory experiments or on-sky telescope verification tests. In those settings, prediction is performed in discrete-time and in a closed AO control loop. And therefore, the specific temporal response behaviours of deformable mirror (DM) and wavefront sensor (WFS) need to be accounted for. Bandwidth limitations of DM and WFS may degrade the overall AO performance and hence may hold back the potential benefit of optimal prediction. The work of ([5]) already describes this for the reference prediction approach.

1.2 Scope

This paper addresses least-square optimal prediction from an analytical and continuous-time point of view. An analytical expression is derived for the minimum wavefront error variance with an optimal, temporal prediction filter. This predictor is based on present and past wavefront phase values only. The minimum variance expression holds for von Kármán type optical turbulence. Since it is analytical, it clearly shows the behaviour of the residual variance as a function of the key parameters: Greenwood frequency, outer scale, wind speed and time-delay. Since the potentially limiting properties of DM and WFS are not taken into account, the analytical expression can serve as a performance upper bound for the servo-lag error of AO systems in practice. Furthermore, it can be used next to Fried's expression (2) for the reference predictor to quantify the potential benefit of optimal prediction in particular turbulence cases. This benefit can be either in terms of a lower phase variance or an enhanced detector integration time. Besides optimal prediction, the paper gives the analytical expression for the reference predictor under von Kármán optical turbulence. This can be regarded as an extension to Fried's expression (2), which only applies to Kolmogorov turbulence.

1.3 Structure of the paper

In the upcoming sections, a stochastic process model will be derived for the wavefront phase fluctuations based on the von Kármán spectral density (Section 2). This model follows from a factorization of the von Kármán power spectrum. Section 3.1 will show that the stochastic model leads to an analytical expression for both the optimal predictor and the minimum mean square value of the time-delay wavefront error. An extension of the Fried expression for the reference predictor under von Kármán turbulence is given in Section 3.2. The specific case of Kolmogorov turbulence for both predictors is addressed in Section 3.3. Section 4 will analyse the properties of optimal, temporal prediction and relate those to the reference prediction approach. The paper will finish up with an analysis for the 'path-integrated case' (Section 5) and final conclusions.

2 Stochastic process model

2.1 Power Spectral Density

Consider a turbulent atmospheric layer of thickness δh at height h_i and an incident plane wave under a zenith angle ζ . The turbulence is assumed to be stationary, homogeneous and isotropic and is described by the von Kármán model for index-of-refraction fluctuations. The wave distortion after propagation through the thin turbulent layer can be characterised by the covariance function of the wavefront phase fluctuations ([6, 7]) and references therein as:

$$C_\phi(r) = \frac{\Gamma(\frac{7}{6})}{\sqrt{2} \pi^{\frac{5}{3}} \Gamma(\frac{1}{3})} k^2 \delta z C_n^2 \kappa_0^{-\frac{5}{3}} (2\pi \kappa_0 r)^{\frac{5}{6}} K_{\frac{5}{6}}(2\pi \kappa_0 r) \quad (3)$$

where $\Gamma(\frac{7}{6})/(\sqrt{2} \pi^{\frac{5}{3}} \Gamma(\frac{1}{3})) = 0.0363$, $K_{5/6}$ is the modified Bessel function of the second kind of order $5/6$, $\kappa_0 = 1/L_0(h_i)$, $L_0(h_i)$ is the outer scale of the atmospheric turbulent layer, $\delta z = \delta h \sec(\zeta)$, k is the wavenumber and $r = |\mathbf{r}|$. The parameter C_n^2 represents the index-of-refraction structure constant at h_i .

The covariance function $C_\phi(r)$ above is circularly symmetric. Taylor's hypothesis of frozen flow implies that for a turbulence variable $u(\mathbf{r}, t)$ it holds, that the future value at $t + \tau$ can be written as a spatially shifted value at t : $u(\mathbf{r}, t + \tau) = u(\mathbf{r} - \mathbf{v}\tau, t)$. Under this hypothesis the spatial covariance function can be converted to a temporal covariance function for a single point by replacing the spatial variable r by $v\tau$; $C_\phi(\tau) = C_\phi(r)$ with $r = v\tau$. Here the variable $v = |\mathbf{v}_\perp|$ represents the modulus of the wind speed perpendicular to the propagation direction at height h_i .

The Fourier Transform of the temporal covariance function, $\int_{-\infty}^{\infty} C_\phi(\tau) \exp(-i\omega\tau) d\tau$, renders the power spectral density (PSD) of phase fluctuations (see eq. 6.699/12 in [8]):

$$\Phi(\omega) = \frac{4}{3} \sqrt{\pi} \Gamma(\frac{7}{6}) k^2 \delta z C_n^2 \frac{v^{\frac{5}{3}}}{(\omega^2 + \omega_0^2)^{\frac{4}{3}}} \quad (4)$$

where $\frac{4}{3} \sqrt{\pi} \Gamma(\frac{7}{6}) = 2.19$ and $\omega_0 = 2\pi v/L_0$. The frequency ω_0 can be regarded as the angular cut-off frequency in the PSD. The function $\Phi(\omega)$ is double-sided and has unit rad^2/Hz . Equation (4) is also given by ([5]), who derived the PSD following a different route.

Expression (4) can be clarified further. For the case of a single turbulent layer at h_i the Greenwood frequency f_G can be expressed as ([9]):

$$f_G = \left[\frac{2^{\frac{1}{3}} \Gamma(\frac{7}{6})}{3 \pi^{\frac{7}{6}}} k^2 C_n^2(h_i) v^{\frac{5}{3}}(h_i) \delta z \right]^{\frac{3}{5}} \quad (5)$$

where $2^{1/3} \Gamma(7/6)/3 \pi^{7/6} = 0.102$. Inserting f_G into the expression for the PSD (4) gives

$$\Phi(\omega) = \frac{(2\pi f_G)^{\frac{5}{3}}}{(\omega^2 + \omega_0^2)^{\frac{4}{3}}} \quad (6)$$

In the limit of an unbounded outer scale $L_0 \rightarrow \infty$ and therefore $\omega_0 \downarrow 0$, the expression for the power spectral density is reduced to

$$\Phi_{Kol}(\omega) = (2\pi f_G)^{\frac{5}{3}} \omega^{-\frac{8}{3}} \quad (7)$$

This is in fact the power spectral density for the case of Kolmogorov turbulence and is in full agreement with eq.(11) in [1] and with the abstract formalism given in ([10]).

The variance of the uncorrected or primary wavefront phase fluctuations - $C_\phi(r)$ for $r = 0$ in (3) - amounts to:

$$\sigma_{prim}^2 = \frac{3 \Gamma(\frac{5}{6})}{2 \sqrt{\pi} \Gamma(\frac{1}{3})} \left(\frac{f_G}{f_0} \right)^{\frac{5}{3}} \quad (8)$$

where $3 \Gamma(\frac{5}{6})/(2 \sqrt{\pi} \Gamma(\frac{1}{3})) = 0.357$ and $f_0 = \omega_0/(2\pi) = v/L_0$. The primary variance increases with the $5/3$ power of the f_G/f_0 fraction. For Kolmogorov turbulence the variance is unbounded.

2.2 Spectral factor

Modeling the wavefront phase fluctuations as a real, wide-sense stationary random process, $\phi(t)$ can be represented in an innovations model form:

$$\phi(t) = \int_0^\infty h(\tau) \xi(t - \tau) d\tau \quad (9)$$

where ξ is zero-mean white noise process, with auto-covariance function: $R_{\xi\xi}(\tau) = \delta(\tau)$. The causal innovations filter $h(\tau)$ is the impulse response of transfer function $H(s)$, which is the minimum-phase spectral factor of the power spectrum $\Phi(s)$, such that $\Phi(s) = H(s)H(-s)$, see [11]. By taking the Laplace transform of the covariance function (3), $\int_{-\infty}^{\infty} C_\phi(\tau) \exp(-s\tau) d\tau$, the power spectrum $\Phi(s)$ is obtained as

$$\Phi(s) = \frac{(2\pi f_G)^{\frac{5}{3}}}{(-s^2 + \omega_0^2)^{\frac{4}{3}}} \quad (10)$$

This power spectrum (10) obeys the Paley-Wiener criterion. Its minimum-phase spectral factor can be readily found by taking the left-hand side roots of $\Phi(s)$:

$$H(s) = \frac{(2\pi f_G)^{\frac{5}{6}}}{(s + \omega_0)^{\frac{4}{3}}} \quad (11)$$

The impulse response of the spectral factor (11) follows by taking the inverse Fourier transform:

$$h(\tau) = \frac{1}{2\pi} \int_{-\infty}^{\infty} H(i\omega) \exp(i\omega\tau) d\omega = \frac{(2\pi f_G)^{\frac{5}{6}}}{\Gamma(\frac{4}{3})} \tau^{\frac{1}{3}} \exp(-\omega_0\tau) \quad (12)$$

see eq. 3.382/6 in [8]). The impulse response (12) is causal, $h(\tau) = 0$ for $\tau < 0$.

2.3 Related model families

The covariance function of wavefront phase fluctuations (3) belongs to the family of Matérn functions ([12]). In the particular case of the von Kármán model, the Matérn smoothness parameter equals 5/6.

Time series models such as damped fractional Brownian motion or tempered fractionally integrated models ([13]) can be regarded as discrete-time versions of Matérn processes and hence can be representative for von Kármán type phase fluctuations. In accordance with (3), the fractional integration parameter then equals 4/3 and the tempering parameter is determined by ω_0 .

Next to existing, numerical methods to simulate von Kármán type wavefront phase screens - see for example ([14]) - the Matérn type models may add further physical and analytical insight into the stochastic behaviour of wavefront phase time series and fields.

3 Residual time-delay error

3.1 Optimal prediction

To determine the minimum of the mean square time-delay error, the optimal prediction of the phase fluctuations $\phi(t)$ needs to be formulated. Given the overall time-delay Δt of the AO loop, at time instant t the future value $\phi(t + \Delta t)$ is to be predicted based on its time history $\phi(t - \tau)$, with $\Delta t > 0$ and $\tau \geq 0$. Note that the predictor relies on temporal information only. Denoting the predictor as a causal linear, time-invariant (LTI) filter P , the prediction of $\phi(t + \Delta t)$ can be expressed as:

$$\hat{\phi}(t + \Delta t) = \int_0^{\infty} p(\tau) \phi(t - \tau) d\tau \quad (13)$$

Based on the innovations model (9, 12), the optimal prediction filter of $\phi(t)$ over an horizon Δt can be derived, see [11]. The Laplace domain optimal predictor equals:

$$P_{opt}(s) = \frac{1}{H(s)} \int_0^{\infty} h(\tau + \Delta t) \exp(-s\tau) d\tau \quad (14)$$

Inserting the spectral factor (11) and (12) yields:

$$P_{opt}(s) = \frac{1}{\Gamma(\frac{4}{3})} \exp(s\Delta t) \Gamma_u(\frac{4}{3}, (s + \omega_0)\Delta t) \quad (15)$$

where Γ_u is the upper incomplete gamma function: $\Gamma_u(a, x) = \int_x^{\infty} t^{a-1} \exp(-t) dt$. The corresponding minimum of the mean square time-delay error can be written as ([11]):

$$\sigma_{min}^2 = \int_0^{\Delta t} h^2(\tau) d\tau \quad (16)$$

Using (12), this minimum mean square error equals:

$$\sigma_{min}^2 = \frac{1}{\Gamma^2(\frac{4}{3})} \left(\frac{f_G}{2f_0} \right)^{\frac{5}{3}} \gamma_{\ell}\left(\frac{5}{3}, 2\omega_0\Delta t\right) \quad (17)$$

where γ_{ℓ} is the lower incomplete gamma function: $\gamma_{\ell}(a, x) = \int_0^x t^{a-1} \exp(-t) dt$.

3.2 Zero-order prediction under von Kármán turbulence

The main principle of the reference prediction approach in AO systems is to feed the latest (measured) wavefront phase value, with opposite sign, back to the optical wavefield. The resultant phase variance will now be compared to the minimum value (17). In the form of the prediction expression (13), the transfer function of the zero-order predictor is $P_{ref}(s) = 1$, leading to the residual error (1). This is in fact the differenced wavefront phase over an interval Δt . Hence, the von Kármán structure function of wavefront phase fluctuations $D_\phi(r)$ (at $r = v\Delta t$) exactly represents the residual variance of the reference approach. This leads to:

$$\begin{aligned}\sigma_{ref}^2 &= D_\phi(v\Delta t) = 2 [\sigma_{prim}^2 - C_\phi(v\Delta t)] \\ &= \frac{1}{\sqrt{\pi} \Gamma(\frac{4}{3})} \left(\frac{f_G}{f_0} \right)^{\frac{5}{3}} \left[\Gamma(\frac{5}{6}) - 2^{\frac{1}{6}} (\omega_0 \Delta t)^{\frac{5}{6}} K_{\frac{5}{6}}(\omega_0 \Delta t) \right]\end{aligned}\quad (18)$$

where $K_{5/6}$ is the modified Bessel function of the second kind of order $5/6$.

3.3 Case of Kolmogorov Turbulence

The expressions for residual phase error variance (17) and (18) hold for any non-negative value of the time-delay Δt . In practice, the delay will be limited and the product $\omega_0 \Delta t$ will be much smaller than unity, even for a high wind speed and a small outer scale. Evaluation of a series expansion of (17) and (18) for small $\omega_0 \Delta t$ leads to:

$$\sigma_{min}^2 \approx (2\pi f_G \Delta t)^{5/3} [0.753 - 0.941(\omega_0 \Delta t) + \mathcal{O}(\omega_0 \Delta t)^2] \quad (19)$$

$$\sigma_{ref}^2 \approx (2\pi f_G \Delta t)^{5/3} [1.33 - 1.07(\omega_0 \Delta t)^{\frac{1}{3}} + \mathcal{O}(\omega_0 \Delta t)^2] \quad (20)$$

For the specific case of Kolmogorov turbulence, in the limit of $L_0 \rightarrow \infty$ and so $f_0 \downarrow 0$, the expressions for the residual variances reduce to:

$$\lim_{f_0 \downarrow 0} \sigma_{min}^2 = \frac{3}{5 \Gamma^2(\frac{4}{3})} (2\pi f_G \Delta t)^{\frac{5}{3}} \approx 16.1 (f_G \Delta t)^{\frac{5}{3}} \quad (21)$$

$$\lim_{f_0 \downarrow 0} \sigma_{ref}^2 = \frac{3}{5} \frac{\Gamma(\frac{1}{6})}{2^{\frac{2}{3}} \sqrt{\pi} \Gamma(\frac{4}{3})} (2\pi f_G \Delta t)^{\frac{5}{3}} \approx 28.4 (f_G \Delta t)^{\frac{5}{3}} \quad (22)$$

Note that the expression for σ_{ref}^2 is equal to eq. (20) in [1].

So, both residual variances increase with the $5/3$ power of the product $f_G \Delta t$. The minimum wavefront phase error with the optimal predictor is a factor $[\Gamma(\frac{4}{3})\Gamma(\frac{1}{6})]/[2^{\frac{2}{3}}\sqrt{\pi}] = 1.77$ smaller than with the reference approach.

4 Analysis

The optimal predictor (15) is a function of time-delay Δt , wind speed v and outer scale L_0 . It does not depend on for instance the wavenumber k , zenith angle ζ or the index-of-refraction structure constant C_n^2 .

From (8), (17) and (18) it follows that the minimum of the mean square time-delay error increases with Δt and decreases with f_0 . Similar to the primary variance and the residual phase variance with the reference approach, the minimum variance grows with the $5/3$ power of the Greenwood frequency. In addition, the normalised residual variance (σ^2/σ_{prim}^2) is a function of the product $f_0 \Delta t$, for both the optimal predictor and the reference predictor.

The optimal predictor always performs better than the reference; see Figures 1, and 2. For small values of $f_0 \Delta t$, the improvement on phase variance reduction ranges from a factor 1.19 (for $f_0 \Delta t = 0.05$) up to 1.77 for $f_0 \Delta t = 0$, which represents the Kolmogorov turbulence case. For large $f_0 \Delta t$, the optimal predictor becomes ineffective and achieves no phase error reduction (for $f_0 \Delta t > 0.4$). For the reference predictor, a large $f_0 \Delta t$ value (> 0.75) leads to doubling of the primary variance, as phase disturbance values large Δt apart are fully uncorrelated; see Figure 2. Note, that these large $f_0 \Delta t$ values are unlikely in practical cases.

Apart from a smaller temporal wavefront error, another benefit of optimal prediction in AO systems would be to allow for a longer detector integration time and therefore the use of a fainter reference star. This was proposed in for instance ([15]) and discussed in further detail in ([16]). With the analytical expressions for the residual variance, (21) and (22) in

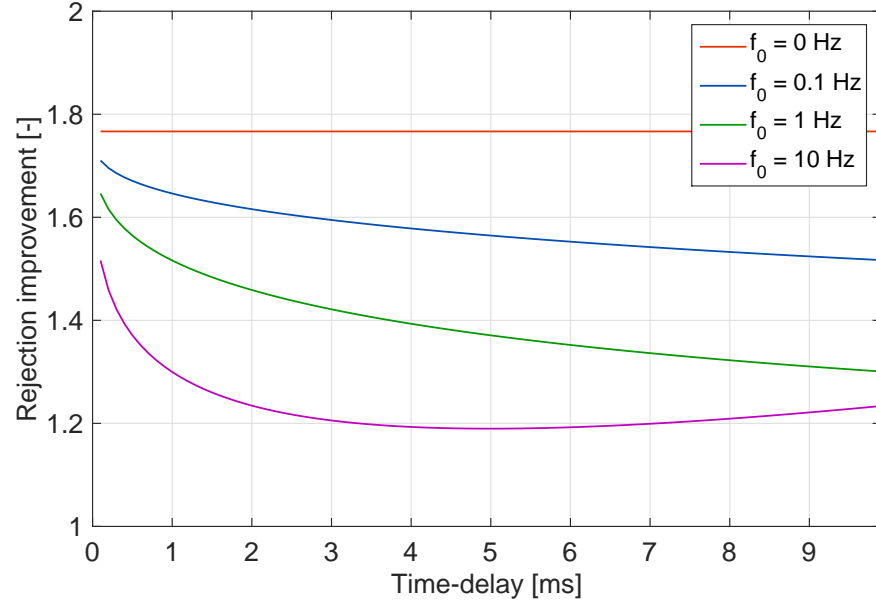


Figure 1: Improvement on variance reduction of predictor versus reference ($\sigma_{ref}^2/\sigma_{min}^2$) for small time-delays and various values of f_0 .

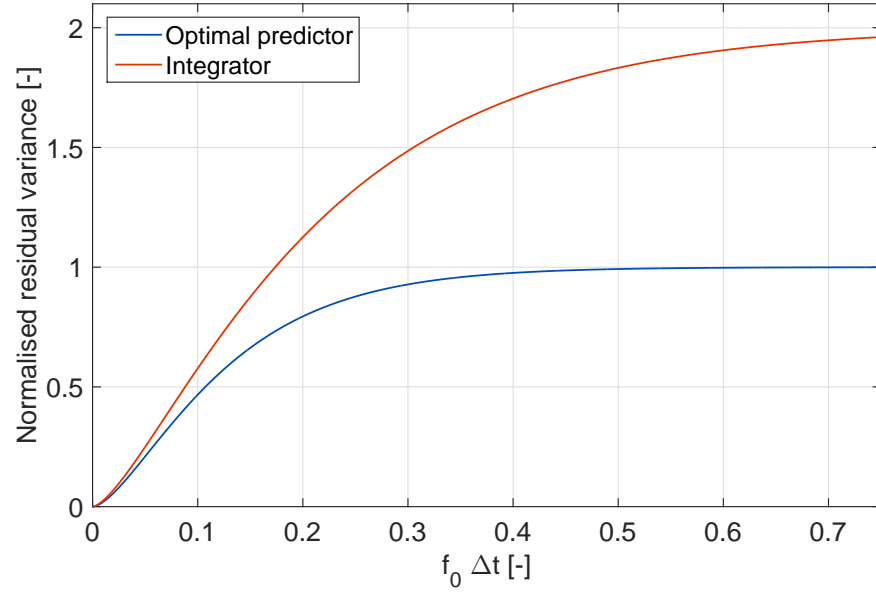


Figure 2: Normalised residual phase variances $\sigma_{min}^2/\sigma_{prim}^2$ and $\sigma_{ref}^2/\sigma_{prim}^2$ against $f_0 \Delta t$.

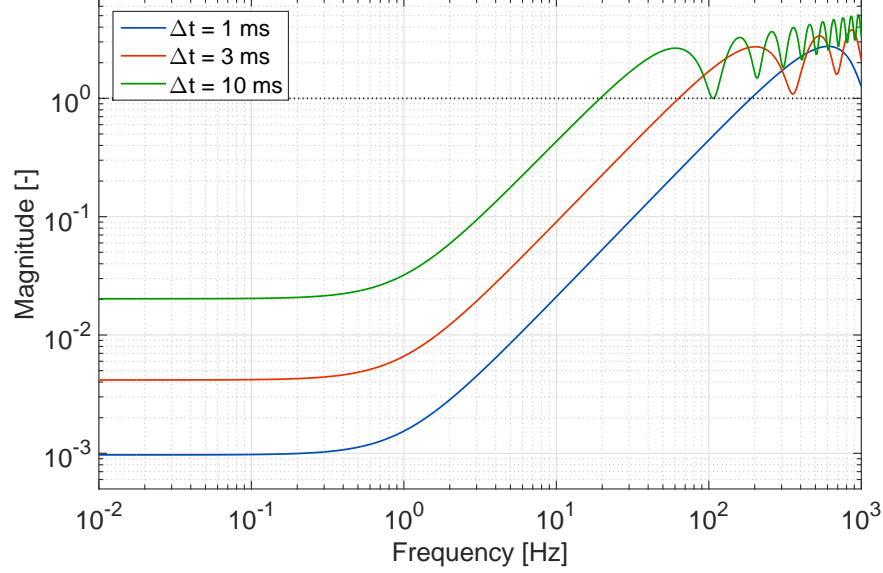


Figure 3: Optimal predictor sensitivity function for $f_0 = 1$ Hz and various values of Δt .

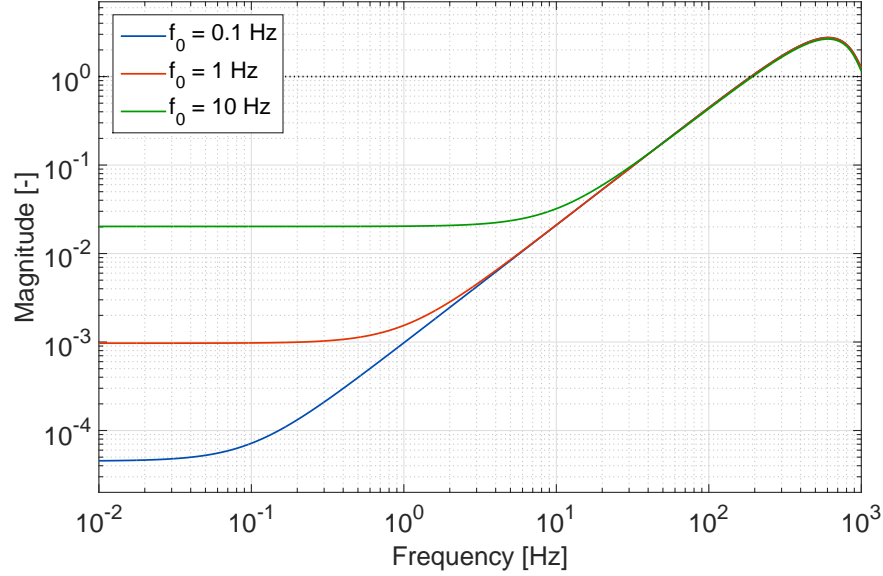


Figure 4: Optimal predictor sensitivity function for $\Delta t = 1$ ms and various values of f_0 .

the Kolmogorov case, the exact gain in integration time can now be quantified. Equalling the two variances gives the following relation between the delay times:

$$\Delta t_{opt} = \left[\frac{\Gamma(\frac{4}{3})\Gamma(\frac{1}{6})}{2^{\frac{2}{3}}\sqrt{\pi}} \right]^{\frac{3}{5}} \Delta t_{ref} \approx 1.41 \Delta t_{ref} \quad (23)$$

So the detector integration time with an optimal predictor can be 1.41 times longer compared to the reference case. This would allow a higher reference star magnitude and would improve the sky coverage.

The spectral behaviour of optimal prediction is shown in Figures 3 and 4, which reveal the modulus of the transfer function from input phase error to residual error (i.e. the sensitivity function). Figure 3 shows that the bandwidth of rejection reduces with the time-delay. The sensitivity curve crosses the unity magnitude line at approximately $(1/5\Delta t)$ Hz. For a fixed time-delay, the bandwidth of rejection is independent of the cut-off frequency f_0 . Only the degree of low-frequency attenuation is affected by f_0 ; see Figure 4. In terms of the PSD of residual phase fluctuations the optimal

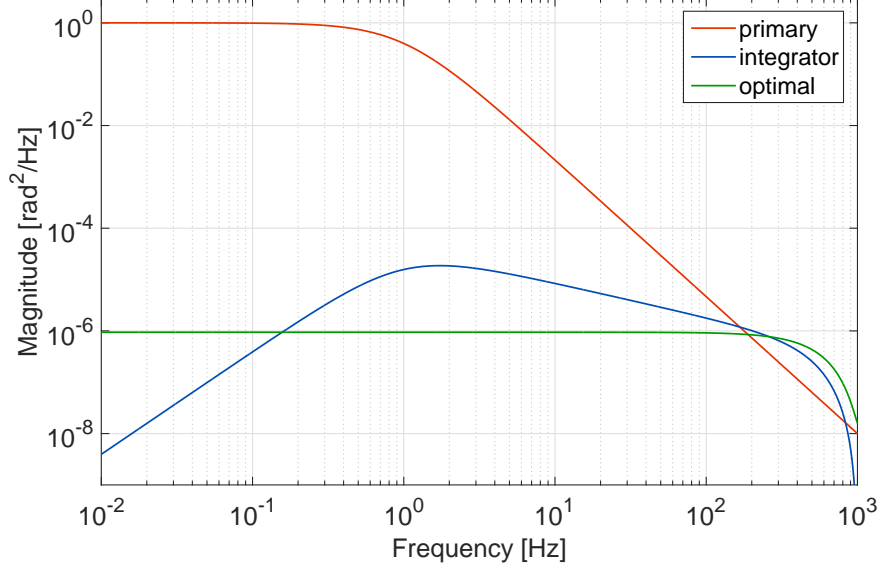


Figure 5: Power Spectral Density of phase fluctuations for the uncorrected case, the reference and the optimal predictor for $\Delta t = 1$ ms and $f_0 = 1$ Hz.

predictor achieves a flat spectrum over a large frequency band. It outperforms the reference in the mid-frequency range, whereas the reference obtains a higher rejection in the very low-frequency range; see Figure 5. Both approaches have about the same frequency bandwidth of rejection and give rise to an increase of the high-frequency phase error.

5 Path-integrated turbulence

So far the analysis of residual wavefront errors has been restricted to propagation through a single, thin layer of turbulence. The atmosphere for the overall propagation path can be viewed as built up from multiple turbulent layers at different heights. For a plane wave and under the geometrical optics approximation, the path-integrated power spectrum of wavefront phase fluctuations $\bar{\Phi}(\omega)$ can then be written as ([6]):

$$\bar{\Phi}(\omega) = \frac{4}{3} \sqrt{\pi} \Gamma\left(\frac{7}{6}\right) k^2 \int_L dz C_n^2(z) \frac{v^{\frac{5}{3}}(z)}{(\omega^2 + \omega_0^2(z))^{\frac{4}{3}}} \quad (24)$$

in which L is the propagation path. Here, the PSD cut-off frequency ω_0 is a function of height, since both the outer scale L_0 and the wind vector \mathbf{v} are height-dependent. In fact, each turbulent layer has its own, specific PSD cut-off frequency. This prevents getting a similar compact form for the overall power spectrum as in (4) for a single layer. This phenomenon was already discussed in detail in ([10]).

Following the approach proposed by several authors ([7, 6, 17]), an effective cut-off frequency $\bar{\omega}_0$ can be used instead. The $\bar{\omega}_0$ value is then set such as to minimise the discrepancy between the true and approximated power spectrum for instance. This metric can be quantified as:

$$\epsilon(\omega_c) = \int_{-\infty}^{\infty} d\omega [\bar{\Phi}(\omega, \omega_c) - \bar{\Phi}(\omega)]^2 \quad (25)$$

where $\bar{\Phi}(\omega, \omega_c)$ is $\bar{\Phi}(\omega)$ of eq. (24) with $\omega_0(z)$ replaced by the constant ω_c . The optimal value of ω_c for which $\epsilon(\omega_c)$ is minimised is denoted as $\bar{\omega}_0$. With the optimal value of the effective cut-off frequency in place, the path-integrated wavefront phase (24) PSD becomes:

$$\bar{\Phi}(\omega) = \frac{(2\pi \bar{f}_G)^{\frac{5}{3}}}{(\omega^2 + \bar{\omega}_0^2)^{\frac{4}{3}}} \quad (26)$$

in which \bar{f}_G is the Greenwood frequency for the integrated path. It can be evaluated by: $(\bar{f}_G)^{\frac{5}{3}} = \int_L f_G^{\frac{5}{3}}(z) dz$.

Now, the power spectrum (26) has exactly the same form as for the single layer case (6). And therefore, the full performance analysis of optimal and reference prediction (section 4) also holds for the approximated path-integrated case with multiple turbulent layers. Note that for Kolmogorov turbulence specifically, the results of section 4 are still exact as then the cut-off frequency ω_0 plays no role.

6 Conclusion

Analytical expressions for the minimum time-delay induced wavefront phase error and the optimal predictor have been presented, under temporal prediction filtering. The specific performance and spectral properties have been analysed. In comparison to the reference zero-order predictor, the performance gain of optimal prediction can be significant. In more detail, the gain depends on the very product of time-delay, wind speed and the reciprocal of outer scale $v\Delta t/L_0$. The largest performance advantage is obtained for small values of $v\Delta t/L_0$ ($< 10^{-3}$). For larger values – up to $v\Delta t/L_0 = 0.2$ – the performance gain is modest.

The optimal performance results can be viewed as an upper bound for practical, discrete-time implementations of predictive control in AO systems.

References

- [1] David L Fried. Time-delay-induced mean-square error in adaptive optics. *JOSA A*, 7(7):1224–1225, 1990.
- [2] John W Hardy. *Adaptive optics for astronomical telescopes*, volume 16. Oxford University Press, 1998.
- [3] Randall N Paschall and David J Anderson. Linear quadratic gaussian control of a deformable mirror adaptive optics system with time-delayed measurements. *Applied optics*, 32(31):6347–6358, 1993.
- [4] Caroline Kulcsár, H.-F Raynaud, Jean-Marc Conan, Rémy Juvénal, and Carlos Correia. Towards minimum-variance control of ELTs AO systems. In *Proceedings of AO4ELT5 Conference*, 2017.
- [5] Patrick M Harrington and Byron M Welsh. Frequency-domain analysis of an adaptive optical system’s temporal response. *Optical Engineering*, 33(7):2336–2343, 1994.
- [6] Larry C Andrews and Ronald L Phillips. *Laser beam propagation through random media*, volume 152. SPIE press Bellingham, WA, 2005.
- [7] Rodolphe Conan. Mean-square residual error of a wavefront after propagation through atmospheric turbulence and after correction with zernike polynomials. *JOSA A*, 25(2):526–536, 2008.
- [8] Izrail Solomonovich Gradshteyn and Iosif Moiseevich Ryzhik. *Table of integrals, series, and products*. Academic press, Cambridge, MA, 2007.
- [9] Darryl P Greenwood. Bandwidth specification for adaptive optics systems. *JOSA*, 67(3):390–393, 1977.
- [10] Jean-Marc Conan, Gérard Rousset, and Pierre-Yves Madec. Wave-front temporal spectra in high-resolution imaging through turbulence. *JOSA A*, 12(7):1559–1570, 1995.
- [11] Athanasios Papoulis and S Unnikrishna Pillai. *Probability, random variables, and stochastic processes*. Mc-Graw Hill, 1991.
- [12] Bertil Matérn. *Spatial Variation: Stochastic Models and Their Application to Some Problems in Forest Surveys and Other Sampling Investigations*. Statens skogsforskningsinstitut, 1960.
- [13] Farzad Sabzikar, Mark M Meerschaert, and Jinghua Chen. Tempered fractional calculus. *Journal of Computational Physics*, 293:14–28, 2015.
- [14] François Assémat, Richard W Wilson, and Eric Gendron. Method for simulating infinitely long and non stationary phase screens with optimized memory storage. *Optics express*, 14(3):988–999, 2006.
- [15] Niek J. Doelman, Karel J. G. Hinnen, Freek J. G. Stoffelen, and Michel H.G. Verhaegen. Optimal control strategy to reduce the temporal wavefront error in AO systems. In Domenico Bonaccini Calia, Brent L. Ellerbroek, and Roberto Ragazzoni, editors, *Advancements in Adaptive Optics*, volume 5490, pages 1426 – 1437. International Society for Optics and Photonics, SPIE, 2004.
- [16] Karel Hinnen, Niek Doelman, and Michel Verhaegen. H2 -optimal control of an adaptive optics system: Part II, closed-loop controller design. In Robert K. Tyson and Michael Lloyd-Hart, editors, *Astronomical Adaptive Optics Systems and Applications II*, volume 5903, pages 86 – 99. International Society for Optics and Photonics, SPIE, 2005.

- [17] VP Lukin, EV Nosov, and BV Fortes. The efficient outer scale of atmospheric turbulence. In *European Southern Observatory Conference and Workshop Proceedings, Astronomy with adaptive optics: present results and future programs, ESO/OSA topical meeting, Sonthofen, Germany*, volume 56, page 619, 1999.